



Post-Earthquake Liquefaction Vulnerability Mapping by Swedish Weight Sounding and Standard Penetration Test

Irdhiani^{1, 2}, Ahmad Rifa'i^{1*} , Teuku Faisal Fathani¹ , Agus Darmawan Adi¹

¹ Department of Civil and Environmental Engineering, Faculty of Engineering, Universitas Gadjah Mada, Yogyakarta 55281, Indonesia.

² Department of Civil Engineering, Faculty of Engineering, Universitas Tadulako, Central Sulawesi Province, 94118, Indonesia.

Received 14 March 2024; Revised 13 June 2024; Accepted 19 June 2024; Published 01 July 2024

Abstract

On September 28, 2018, a 7.5-magnitude earthquake struck Palu City, Sigi Regency, and Donggala Regency in Central Sulawesi. It triggered liquefaction in different locations, including Balaroa, Petobo, Jono Oge, and Sibalaya; Typically, a significant number of studies conducted in the Balaroa region relied on a small amount of field test data to cover a rather large area. This research aims to map the liquefaction vulnerability by analyzing the data from both the Swedish Weight Sounding (SWS) and the Standard Penetration Test (SPT) in the Balaroa area. The SWS data was acquired through mapping using a systematic grid sampling method at ten different locations. The liquefaction potential was analyzed based on the N values by converting the SWS data (N_{sw} and W_{sw}) to N values using the Inada equation (1960). Afterward, the analysis findings were verified by comparing them with the SPT data obtained from the same area. Based on the SWS and SPT data analysis results, all locations, including the adjacent areas, exhibited very high liquefaction vulnerability. In contrast, the SPT data indicated that the areas further from the spots exhibited low and very low liquefaction. The findings indicated that the occurrence of post-earthquake liquefaction in Balaroa and other regions within Palu City is prone to recurrence following earthquakes of specific magnitudes.

Keywords: Liquefaction Vulnerability; Ground Acceleration; Safety Factor; Swedish Weight Sounding; Standard Penetration Test.

1. Introduction

Central Sulawesi, a province in Indonesia, is prone to high-magnitude earthquakes. On September 28, 2018, at 06.02 p.m., a 7.5-magnitude earthquake mostly affected Donggala Regency, located 80 km northwest of Palu City. It also impacted Palu City and Sigi Regency [1]. Figure 1 displays the epicenter and distribution of ground shaking as measured by the MMI (Modified Mercalli Intensity) scale and reported by the USGS (United States Geological Survey). The distribution map shows that the ground shaking in Palu City reached intensity IX on the MMI scale [2]. The earthquake resulted in significant structural damage to buildings and induced liquefaction, leading to numerous casualties. Liquefaction occurred in Petobo and Balaroa villages in Palu City, as well as in Jono Oge and Sibalaya villages in Sigi Regency.

Liquefaction is the process by which granular deposits lose their strength and stiffness and transition from a solid to a liquid state due to an increase in pore water pressure during seismic waves [3]. Liquefaction is most likely to happen in areas prone to earthquakes, where there are water-saturated and low-density sand deposits, and when the seismic waves exceed certain threshold values [4]. This phenomenon is an aftermath of earthquakes in areas with unconsolidated

* Corresponding author: ahmad.rifai@ugm.ac.id

 <http://dx.doi.org/10.28991/CEJ-2024-010-07-09>



© 2024 by the authors. Licensee C.E.J, Tehran, Iran. This article is an open access article distributed under the terms and conditions of the Creative Commons Attribution (CC-BY) license (<http://creativecommons.org/licenses/by/4.0/>).

sand and a shallow water table (< 9.0 m). It is affected by the intensity, duration, and proximity to the epicenter of seismic waves. Liquefaction-prone sandy soil layers are typically found in geologically restricted areas. Liquefaction commonly occurs in areas with alluvial fan deposits, alluvial plains, coasts, former lakes, and estuaries [5, 6].

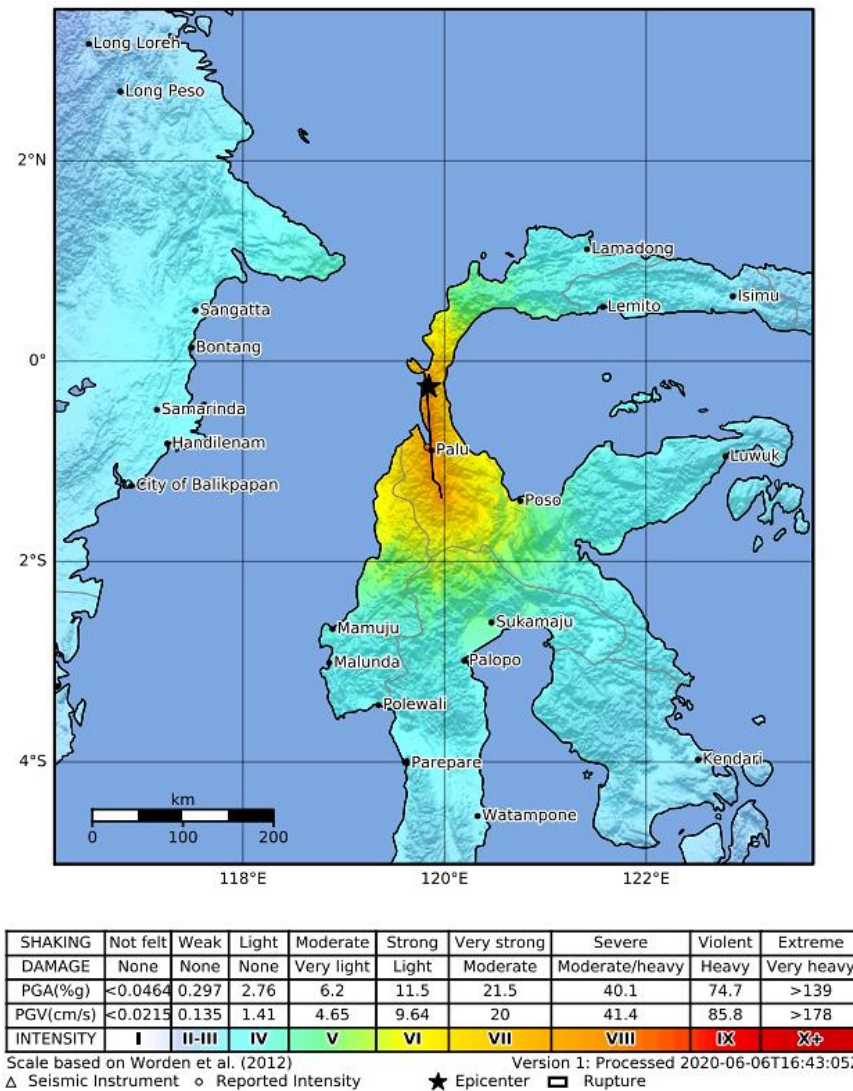


Figure 1. Map of the epicenter location and earthquake intensity distributions measured on the MMI scale (modified from [7])

Extensive research has been conducted on liquefaction in Palu City, located in the Central Sulawesi Province, as well as in several other provinces and countries, including those with a wide range of topics and areas of investigation. Multiple investigations on liquefaction in Balaroa after the Palu earthquake in 2018 encompassed surveys and observations of geotechnical damages [2, 8–11], evaluations of liquefaction potential using SPT data [12–14], CPT (Cone Penetration Test) and shear wave velocity (V_s) data [15], and microtremor data [16, 17]. Although liquefaction potential research using SWS data had been conducted at six locations in Balaroa [18], the availability of SWS technologies in Indonesia remains severely limited, thus resulting in insufficient research conducted using these tools. The commonly employed soil investigations in Indonesia are the Standard Penetration Test (SPT) and Cone Penetration Test (CPT). Furthermore, many researchers have used the data obtained from SPT and CPT results to determine the liquefaction potential. The tests require considerable resources, including skilled operators, supporting equipment, and larger budgets; nevertheless, this research used cost-effective and portable SWS data. The SWS device was operated manually. It had a relatively effective ability to penetrate and was capable of exploring depths of up to 10 meters. Typically, a significant number of studies conducted in the Balaroa region relied on a small amount of field test data to cover a rather large area. This research mapped the liquefaction potential using the SWS and SPT data [19]. The liquefaction potential was analyzed based on the N values by converting the SWS data (N_{sw} and W_{sw}) to N values using the Inada equation (1960). Afterward, the results were verified by comparing them with the SPT data in the same location.

2. Literature Review

The Swedish Weight Sounding (SWS) test was initially introduced and recommended in Sweden in 1917. It has since been used for conducting field surveys of subsurface profiles beneath railroads. Since then, the SWS test method has gained extensive use in Sweden, Norway, Finland, and Denmark. In 1954, the SWS test method was initially utilized in Japan to conduct field surveys of river embankments. Over time, it was expanded to include field surveys of road construction. In 2001, the Ministry of Land, Infrastructure, and Transport in Japan officially recommended the SWS test method as a means to estimate the permissible shear strength of soil for residential construction [20]. The SWS test has been implemented in various Eastern European nations, as well as in Singapore and Algeria [21]. It was used to calculate the required foundation depth and bearing capability for multiple buildings located in the southern area of Tehran, Iran [22].

An empirical correlation was established between the number of N -SPT strokes and that of N_{sw} half-turns from the SWS test. This correlation closely resembled the one proposed by Inada, indicating that a similar correlation could be applied in the Philippines with minor adjustments [23]. Research conducted at the University of Sheffield, UK, analyzed the liquefaction potential in residential dwellings, using Swedish Weight Sounding (SWS) at 7 places in a sandbox with dimensions of 40 m length, 6 m width, and 5 m depth. Based on the SWS data, the factor of safety was lower while the LPI value was higher compared to the SPT data [24]. The soil types were classified based on the sound pressure level (SPL) measured using Swedish Weight Sounding (SWS) equipment in the vicinity of the site. The complete tests include SWS and SPT at four different locations. Additionally, sieve analysis was performed at two different locations. Based on the suggested SWS test, the accuracy of soil classification was lower compared to that of SPT despite being considered sufficient for residential soil surveys at a reduced cost [25]. The soil collapses that occurred in Lokanthali along the Araniko Highway in Kathmandu as a result of the 7.8-magnitude Gorkha earthquake in 2015 were detected using the Swedish Weight Sounding (SWS) test, Vane Shear Test (VST), and topographic mapping. Additionally, numerical research was conducted to get insight into the seismic susceptibility of the location. According to the study, Lokanthali experienced landslides caused by seismic activity, despite having gentle slopes and being subjected to mild ground accelerations during the Gorkha Earthquake [26].

3. Research Methodology

3.1. Research Framework

This research commenced by examining general information about the location, geological maps, topographic maps, and aerial images of the liquefaction-afflicted area, Balaroa. In addition, the liquefaction potential was analyzed by using field data of SPT and SWS. The liquefaction potential analysis yielded a safety factor (SF), which is the ratio of Cyclic Resistance Ratio (CRR) to Cyclic Stress Ratio (CSR) by which the liquefaction potential index (LPI) value could then be derived. The liquefaction potential at each testing location was analyzed based on their geographical coordinates and then mapped using ArcGIS software. The research methodology implemented is illustrated in Figure 2.

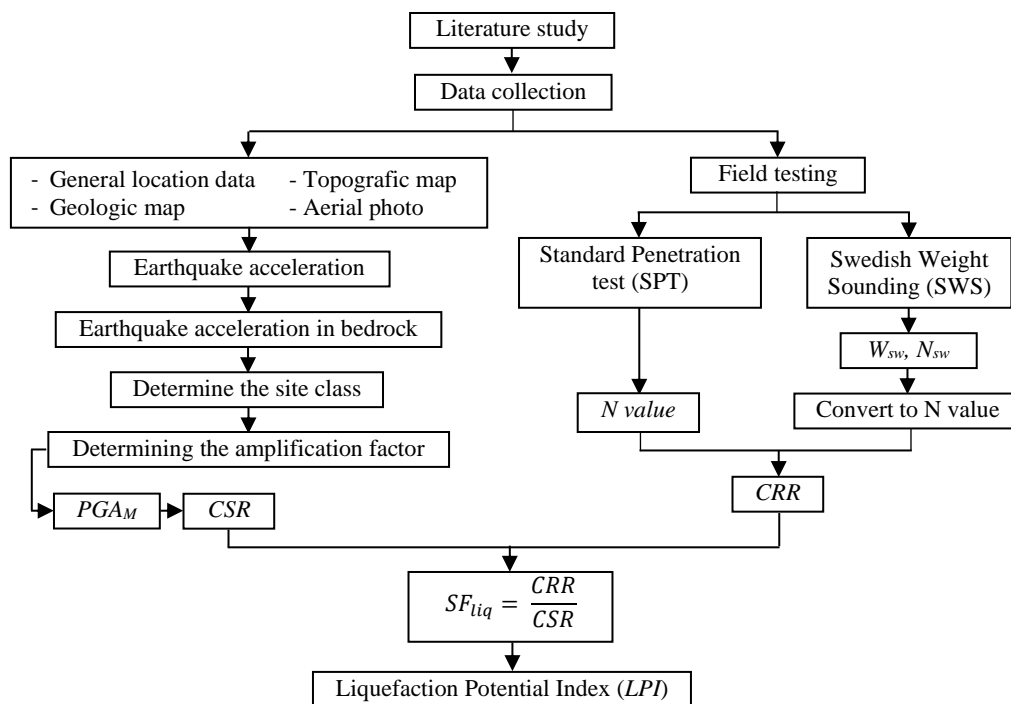


Figure 2. Flowchart of Research

3.2. Study Area

This research was conducted in Balaroa, an area situated in the western part of Palu City. Balaroa is the sole location along the west coast of the Palu River that is experiencing liquefaction. It is near the Palu-koro fault (approximately 100 m). Hence, the intensity varied amongst Petobo, Jono Oge, Sibalaya, and Lolu [1]. In addition, the Balaroa area has a comparatively more pronounced incline in its terrain compared to Petobo and Jono Oge, with the geological gradient ranging from 2% to 5% [1].

Balaroa covers an area of approximately 203,042 ha comprising 85% plain and 15% hills with 15 m in elevation [27]. Following the occurrence of the Palu earthquake in 2018, numerous buildings located approximately 1 km to the west of the Palu-Koro fault sustained significant damage. The damages included properties and roadways, affecting an area of approximately 34.5 ha with a radius of 2.5 km [1], an additional area of 38 ha [2], and a width of 0.4 km² [10]. The initial slope between *crown* and *toe* was roughly 3° [2], and less than 5% [28]. Figure 3 demonstrates the Balaroa area before and after the 7.5-*M_w* earthquake in 2018 and the condition of Balaroa in October 2002 [29].

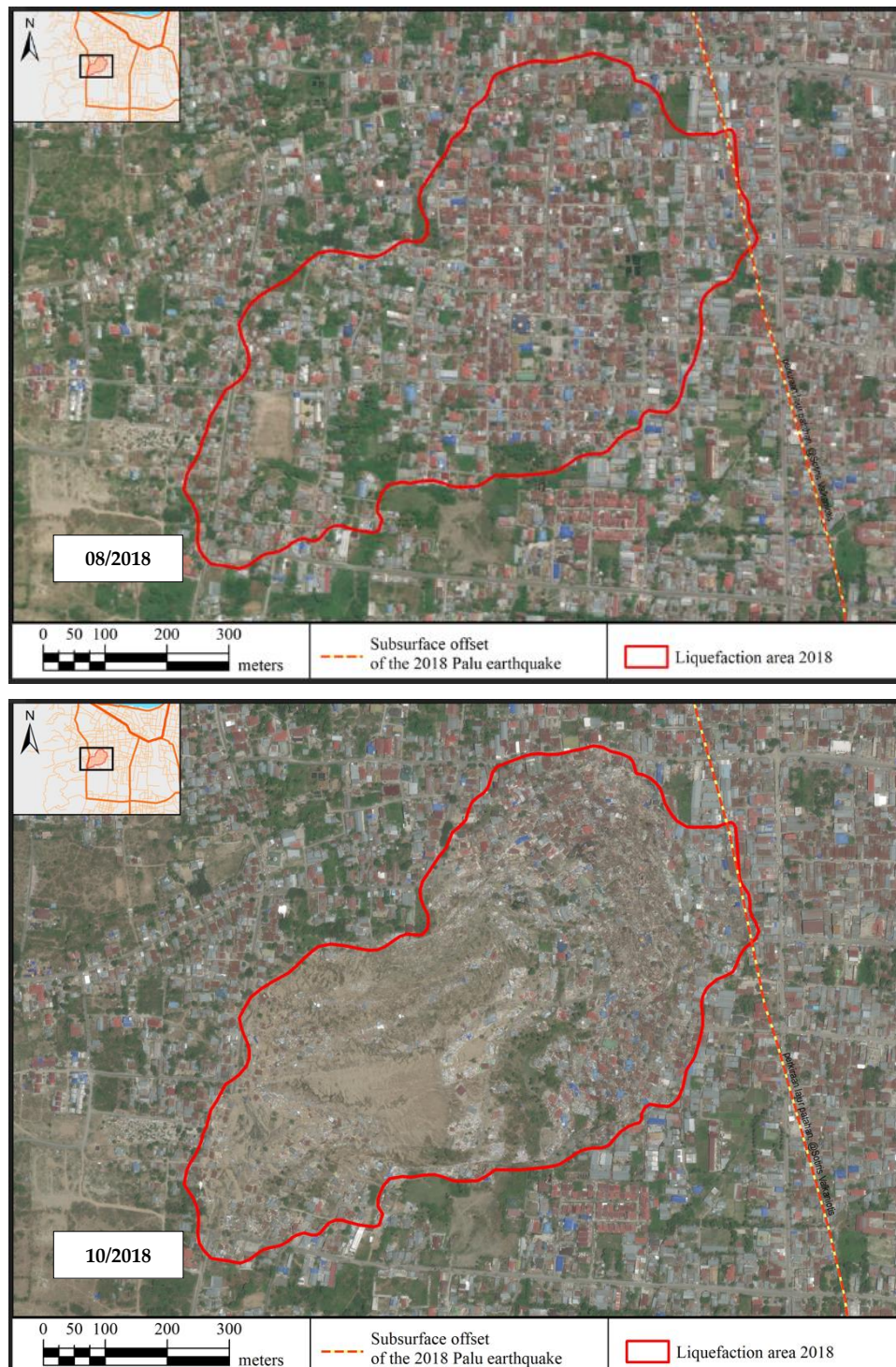




Figure 3. Balaroa area before and after the 7.5- M_w earthquake; modified from [29]

3.3. The SWS (Swedish Weight Sounding) and SPT (Standard Penetration) Test Location

This research employed geotechnical investigation data obtained after the 7.5 M_w earthquake in the Balaroa area, using the SWS and SPT data. Figure 4 shows the test locations. The SWS data comprised 29 points including 20 points in the liquefaction-affected area (S-01 to S-20), 5 points bordering the liquefaction-affected area (S-21, S-22, S-23, S-24, S-29), and 4 points near the liquefaction-affected area (S-25 to S-28). The SPT data comprised 6 sites, i.e., BH-01 located in the liquefaction-affected area, BH-02 and BH-05 located on the border of the liquefaction-affected area, and BH-03, BH-04, and BH-06 located at a considerable distance from the liquefaction-affected area.

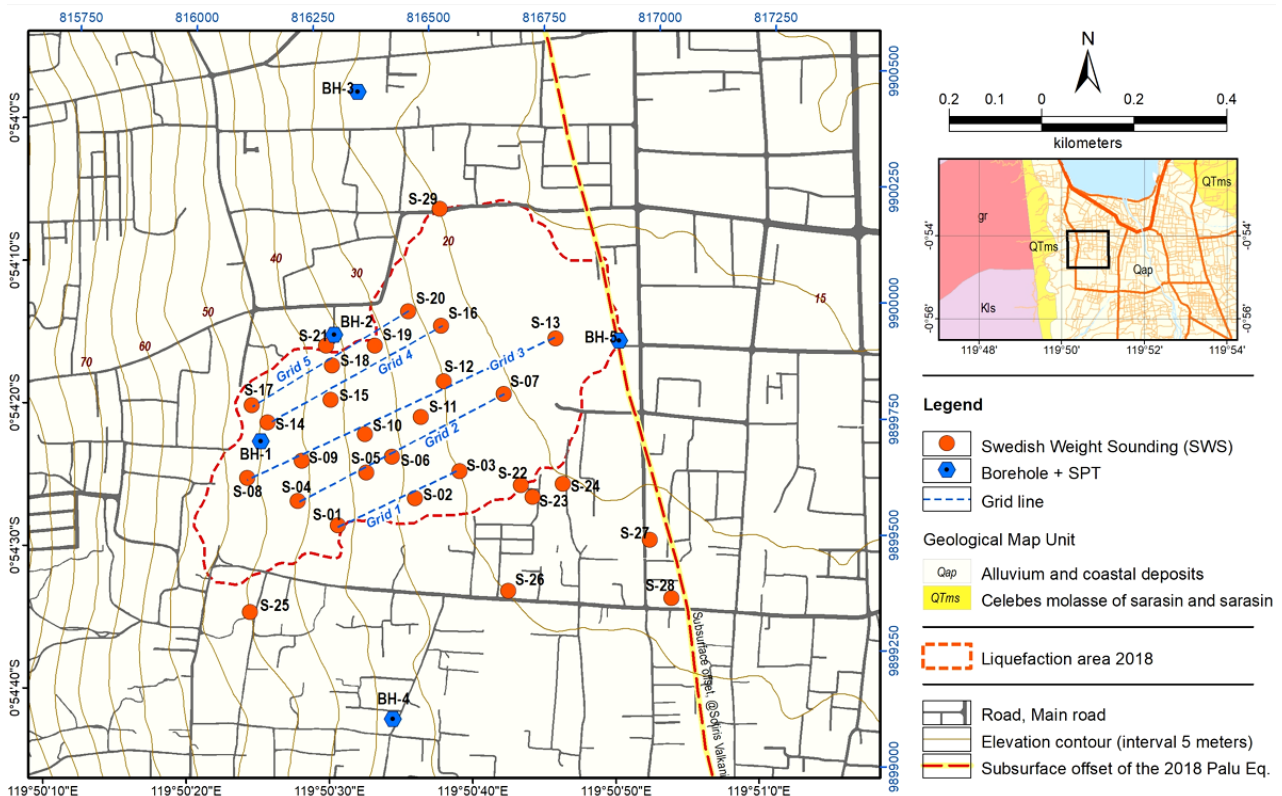


Figure 4. The location of Swedish Weight Sounding and Borehole Test Points

The SWS test on the liquefaction-affected area did not align with the planned grid due to an unsuitable placement. Several points were situated in a marshland abundant with towering vegetation, while others were situated on ground covered with scattered rocks. Due to existing rocks in shallow layers, the test points were relocated by up to 6 points. The grid direction was aligned parallel to the landslide, which extended from west to east. Figure 5 illustrates a specific area in Balaroa that is characterized by the presence of weeds and rocks.



Figure 5. Condition of Balaroa during the examination on June 2023 (a) Area with rocks (b) and (c) Marsh filled with tall grass

3.4. Swedish Weight Sounding (SWS)

The Geotechnical Commission of the Swedish State Railways introduced SWS in 1917 [30, 31]. It is a device to measure the resistance of static soil penetration and assess soil hardness or soil layer composition. As a simple device, it effectively penetrates soil and is suitable for conducting soil surveys with a maximum depth of 10 m. Furthermore, it can be classified as a cost-effective and highly portable on-site examination [32–34]. In addition to its simplicity, this device has a profile with a continuously evolving resistance to penetration, which is useful for stratigraphic interpretation. However, the primary limitation of this instrument is that the user must first convert the acquired data into the penetration resistance equivalent to *N*-SPT or CPT before utilizing it for the liquefaction potential analysis [22].

The study conducted by Tsukamoto et al. [35] examined the methodology for estimating the soil liquefaction resistance (*R_l*) using SWS testing. The proposed procedure was subsequently compared to the conventional one. In a conventional procedure, the evaluation of soil liquefaction resistance completely depends on the *N*-SPT value, as depicted in Figure 6. The empirical formula most frequently used, as suggested by Inada [36], involves measuring the penetration resistance through the SWS test to obtain *W_{sw}* and *N_{sw}* values, which are further converted to *N* values [35].

The *N_{sw}* value obtained from the SWS test is converted to the *N* value by initially identifying the soil. The equations for converting the *N_{sw}* value to *N*, as stated in Inada [36], are as follows.

For sandy soil:

$$N = 2 W_{sw} + 0.067 N_{sw} \tag{1}$$

For cohesive soil:

$$N = 3 W_{sw} + 0.050 N_{sw} \tag{2}$$

where *W_{sw}* = the amount of load in kN unit and *N_{sw}* = number of half turns per 1 meter.

SWS test also serves to gather information on the soil profiles that are affected by liquefaction or landslide, as well as those that are not affected. It also helps to identify the dynamic and static features of soil profiles. Due to its user-friendly interface, this device is frequently employed for investigating the soils in areas affected by seismic activity.

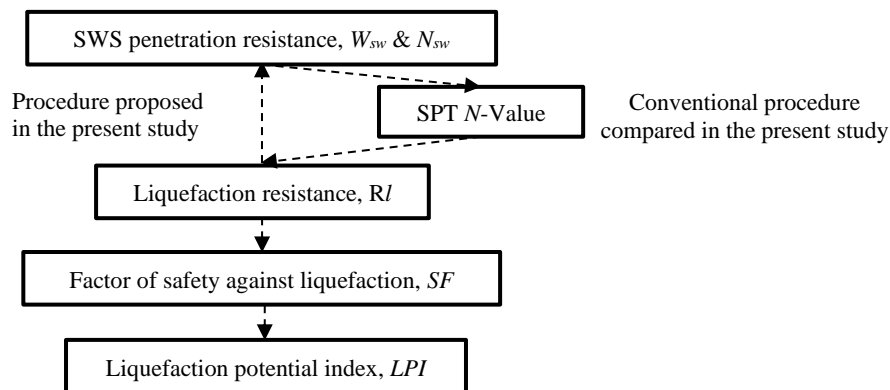


Figure 6. The procedure to estimate the soil liquefaction resistance (*R_l*) as proposed by the conventional procedure

3.5. Liquefaction Potential Analysis

The liquefaction potential was analyzed using the simple method of Idriss-Boulanger based on the SPT (Standard Penetration Test), generating the safety factor against liquefaction [37]. The Idriss-Boulanger method has the minimum weight factor based on the error analysis of the weighted factor. Therefore, this method is the most reliable one to predict liquefaction [38].

CSR (Cyclic Stress Ratio) of Each Soil Layer is a cyclic pressure induced by an earthquake. This pressure affects the liquefaction by 65% of the peak cyclic pressure formulated as follows [38].

$$CSR = 0.65 r_d \frac{a_{max}}{g} \frac{\sigma_{vo}}{\sigma'_{vo}} \quad (3)$$

where r_d = shear stress reduction coefficient, a_{max} = maximum earthquake acceleration in the soil layers (m/s^2), g = gravitational acceleration (m/s^2), σ_{vo} = total vertical pressure of soil layers during consolidation (kN/m^2), and σ'_{vo} = effective vertical pressure of soil layers during consolidation (kN/m^2).

The evaluation of liquefaction using PGA_M value is stated in the following equation.

$$PGA_M = F_{PGA} \cdot PGA \quad (4)$$

where PGA_M = MCE_G of peak soil acceleration adjusted to site classification effect, PGA = mapped peak soil acceleration, and F_{PGA} = site coefficient.

The equation to determine the CSR was obtained by substituting Equation 4 with Equation 3 as follows.

$$CSR = 0.65 r_d \left(\frac{\sigma_{vo}}{\sigma'_{vo}} \right) PGA_M \quad (5)$$

CRR (Cyclic Resistance Ratio) is a parameter of soil resistance to withstand the CSR cyclic weight. Idriss and Boulanger [37] modified the values of several parameters, such as $(N_1)_{60}$, $\Delta(N_1)_{60}$, and $CRR_{7.5}$ summarized into the following equations:

$$(N_1)_{60cs} = (N_1)_{60} + \Delta(N_1)_{60} \quad (6)$$

$$\Delta(N_1)_{60} = \exp\left(1.63 + \frac{9.7}{FC + 0.01} - \left(\frac{15.7}{FC + 0.01}\right)^2\right) \quad (7)$$

$$CRR_{M=7.5 \& \sigma'_{vc}=1} = \exp\left(\frac{(N_1)_{60cs}}{14.1} + \left(\frac{(N_1)_{60cs}}{126}\right)^2 - \left(\frac{(N_1)_{60cs}}{23.6}\right)^3 + \left(\frac{(N_1)_{60cs}}{25.4}\right)^4 - 2.8\right) \quad (8)$$

Safety factor (SF) against liquefaction was applied after obtaining the CSR and CRR values expressed by the following equation:

$$FS = \frac{CRR}{CSR} \quad (9)$$

If SF (Safety Factor) is less or equal to one ($FS \leq 1.0$), soil liquefaction occurs. If SF is more than one ($FS > 1.0$), soil liquefaction does not occur.

3.6. Liquefaction Potential Index (LPI)

LPI is a quantitative measure used to estimate the level of liquefaction vulnerability that occurs in an area. The LPI calculation was limited to the depth ranging between 0 and 20 m beneath the soil surface. The LPI value calculation for the soil layer with a depth of less than 20 m can be determined using the equation proposed by Luna and Frost [39] in the following equation:

$$LPI = \sum_{i=1}^n W_i F_i H_i \quad (10)$$

where $F = 1 - SF$ for $FS \leq 1.0$, $F = 0$ for $FS > 1.0$, W = weight function dependent on depth, up to $10 - 0.5 z$, and H = layer thickness.

Liquefaction with high damage levels occurred in locations with $LPI > 15$ [40–42]. Previous studies [40–44] compiled liquefaction cases and compared the LPI with the damages caused by the liquefaction. The LPI values were used to draw a map of liquefaction potential in Charleston, South Carolina, based on the history of the 1886 earthquake [45]. Table 1 shows the classification of LPI based on the risk of liquefaction potential.

Table 1. Classification of Liquefaction Vulnerability [36-38]

<i>LPI</i> Value	Liquefaction Potential Level
$LPI = 0$	Very Low
$0 < LPI \leq 5$	Low
$5 < LPI \leq 15$	High
$15 > LPI$	Very High

4. Results and Discussion

4.1. Site Classification of Balaroa Area

The site classification of Balaroa was established according to the guidelines outlined in Hayati & Andrus [45] and SNI-1726-2019 [46]. It was used to ascertain the value of *PGA* (Peak Ground Acceleration) amplification based on the earthquake map of the Indonesia region by inputting coordinates and selecting the site classification relevant to respective coordinates. The site classification included SA (hard rocks), SB (stones), SC (hard soils that are very solid with soft rocks), SD (medium soil), SE (soft soil), and SF (particular soil requiring specific geotechnical investigation). It was also classified based on \bar{N} value. The \bar{N} values distributed on SWS test locations were used to establish the site classification, which was subsequently validated by comparing it with the site classification determined by the SPT test on the adjacent test points. The values were obtained by converting N_{sw} values through the process of soil identification.

The \bar{N} values from the SWS test were lower than \bar{N} values of the SPT test. This aligns with the findings of the study of Armario et al. [23], indicating that the empirical equation presented by Inada (1960) generates a very low equivalent *N* value. The SWS test yielded $\bar{N} < 15$ for all points while the SPT test obtained BH-01 and BH-05. Therefore, the sites were classified as soft soils (SE). Meanwhile, the \bar{N} value ranging from 15 to 50, indicating medium soil (SD), was obtained using the SPT test at various points located both distant from and near the liquefaction-affected area. These points included BH-03, BH-04, BH-06, and the adjoining BH-02.

4.2. Peak Ground Acceleration (PGA)

The *PGA* for each test point was determined according to the guidelines set by the Ministry of Public Works and Public Housing of the Republic of Indonesia. It was based on the information provided on the website of Indonesian Spectra Design in 2021 [47]. The *PGA* value was obtained by inputting the coordinates of each test location in the earthquake map of the Indonesia region. This number represents the acceleration in bedrock; meanwhile, the *PGA* value on the surface was influenced by the amplification factor value (F_{PGA}). The soil site classification has an impact on the *PGA* and F_{PGA} values. These values for each test point can be seen in Table 2.

4.3. The Locations of the Water Table and PGA_M Value

Table 2 displays the water table locations, site coordinates, and *PGA* adjusted to the impacts of site classification (PGA_M) for SWS test points. The water tables of S-01 to S-29 were directly measured through SWS test boreholes. The *PGA* for each borehole was determined using the information provided on the Indonesian Spectra Design website in 2021 [47].

The position of the groundwater table is one of the elements that can lead to liquefaction. There is an inverse relationship between the depth of the water table and the liquefaction susceptibility. In other words, the deeper the water table, the more resistant the soil is to liquefaction, and conversely, the shallower the water table, the more susceptible the soil is to liquefaction. Youd [48] asserts that only sediments that are saturated or have a tendency to become saturated are considered to be sensitive to liquefaction. Balaroa has established this criterion, i.e., susceptible to liquefaction, based on findings of Soekamto et al. [49] that the region of Palu City is made up of Holocene-age coastal alluvial deposits (Qap). These deposits consist of gravel, sand, silt, and coral limestone that were generated in river, delta, and shallow marine environments.

The Balaroa's water tables in the liquefaction-affected area were exceptionally shallow, despite the intense heat. Moreover, in other areas, a portion of them remained stagnant on the ground and even elevated above it. According to previous studies conducted in the Balaroa area and the observations made by Rohit et al. [10], it was reported that there was the presence of standing water resulting from subsurface streams after the liquefaction event. Moreover, research findings from Tadulako Geoelectrical Service [50] indicated that the low-level water tables were discovered on all four geoelectric measurement trajectories, running approximately parallel to the north-south and west-east directions in the Balaroa area. It indicated numerous springs were detected at the measurement sites.

All the testing points in the liquefaction-affected area (S-01 to S-021) had water tables with depths ranging from 5 to 55 cm. The water tables in the vicinity of the liquefaction-affected area, specifically sites S-22 to S-24, had depths

ranging from 9 to 43 cm. Concurrently, the water tables at locations S-25 to S-29, which are near the area affected by liquefaction, had depths ranging from 43 to 60 cm. Table 2 displays the water tables for each testing point.

Table 2. The locations of the water table coordinate, and PGA_M values in Balaroa

Site Code	GWL (cm)	Long	Lat	Site Classification	PGA_M (g)
S-01	-27	119.84172	-0.907944	SE	0.58124
S-02	-8	119.84322	-0.907417	SE	0.58018
S-03	-28	119.84408	-0.906889	SE	0.57955
S-04		119.84094	-0.907472	SE	0.58176
S-05		119.84228	-0.906917	SE	0.58084
S-06	-55	119.84278	-0.906611	SE	0.58049
S-07	-38	119.84494	-0.905389	SE	0.57896
S-08		119.83997	-0.907028	SE	0.58244
S-09	-29	119.84103	-0.906694	SE	0.58172
S-10	-35	119.84225	-0.906167	SE	0.58089
S-11	-42	119.84333	-0.905833	SE	0.58014
S-12	-9	119.84378	-0.905139	SE	0.57982
S-13		119.84594	-0.904306	SE	0.57823
S-14	-17	119.84036	-0.905944	SE	0.58222
S-15	-21	119.84158	-0.905500	SE	0.58137
S-16	-24	119.84372	-0.904056	SE	0.57987
S-17		119.84006	-0.905611	SE	0.58240
S-18	-45	119.84161	-0.904833	SE	0.58137
S-20		119.84308	-0.903778	SE	0.58031
S-21		119.84150	-0.904444	SE	0.58141
S-22	-9	119.84528	-0.907167	SE	0.57869
S-23	-43	119.84550	-0.907389	SE	0.57850
S-24	-22	119.84608	-0.907139	SE	0.57088
S-25		119.84003	-0.909639	SE	0.58236
S-26	-43	119.84503	-0.909222	SE	0.57883
S-27	-46	119.84778	-0.908222	SE	0.57677
S-28	-60	119.84819	-0.909361	SE	0.57644
S-29		119.84369	-0.901778	SE	0.57991
BH-01	+1.6	119.84023	-0.906313	SE	0.5809
BH-02	-2.55	119.84165	-0.904234	SD	0.5118
BH-03	+0.1	119.84211	-0.899500	SD	0.6067
BH-04	+0.41	119.84280	-0.911724	SD	0.5094
BH-05	-1.0	119.84718	-0.904347	SE	0.5793
BH-06	-17.26	119.841121	-0.926138	SD	0.5119

4.4. Swedish Weight Sounding (SWS) Test Results

The SWS test resulted in the N_{sw} (N/m) value, which represents the number of half turns per meter, as shown in Figure 6. The tests were limited to penetrations up to a depth of 9.5 m due to the availability of a mere 10 rods, each with a length of 1 m. The N_{sw} value represents the ratio of half turns per meter to the number of penetrations. Soil density increases as the N_{sw} number increases. Based on the SWS tests in Balaroa, there were specific locations where the depth reached a certain point and the N_{sw} value was recorded as zero. Before the rotation of the rod, penetration took place upon the distribution of weight.

The charts in Figure 6 were classified in parallel with the grid lines running from west to east, encompassing points S-01 to S-29. The classification of these grids can be seen in Figure 3. These charts illustrate variations in density across different locations, primarily caused by the presence of rocks that limit the maximum depth to 9.5 m. The 19 testing points with N_{sw} values equal to zero at certain depths were S-01, S-03, S-06, S-07, S-09, S-10, S-11, S-14, S-15, S-16, S-19, S-22, S-23, S-24, S-25, S-26, S-27, S-28 and S-29. The depth varied between 1.5 and 9.5 m. These points were situated within, adjacent, and outside the liquefaction-affected area. Point S-24 had a quite high N_{sw} value in the depth of 1.38 (between 1.25 and 1.5 m) due to an obstacle. The value was high because the number of half-turns reached 50, although with penetration merely reached a depth of 13 cm. The point test S-24 was extended due to the absence of rocks on the screw point. Figure 7 displays 6 test points, namely S-04, S-05, S-13, S-14, S-20, and S-25, all of which have a depth of less than 2 m. A subset of the tests was replicated six times at various locations, deviating from the original intention. Typically, these test spots were impeded by rocks, hindering further penetration.

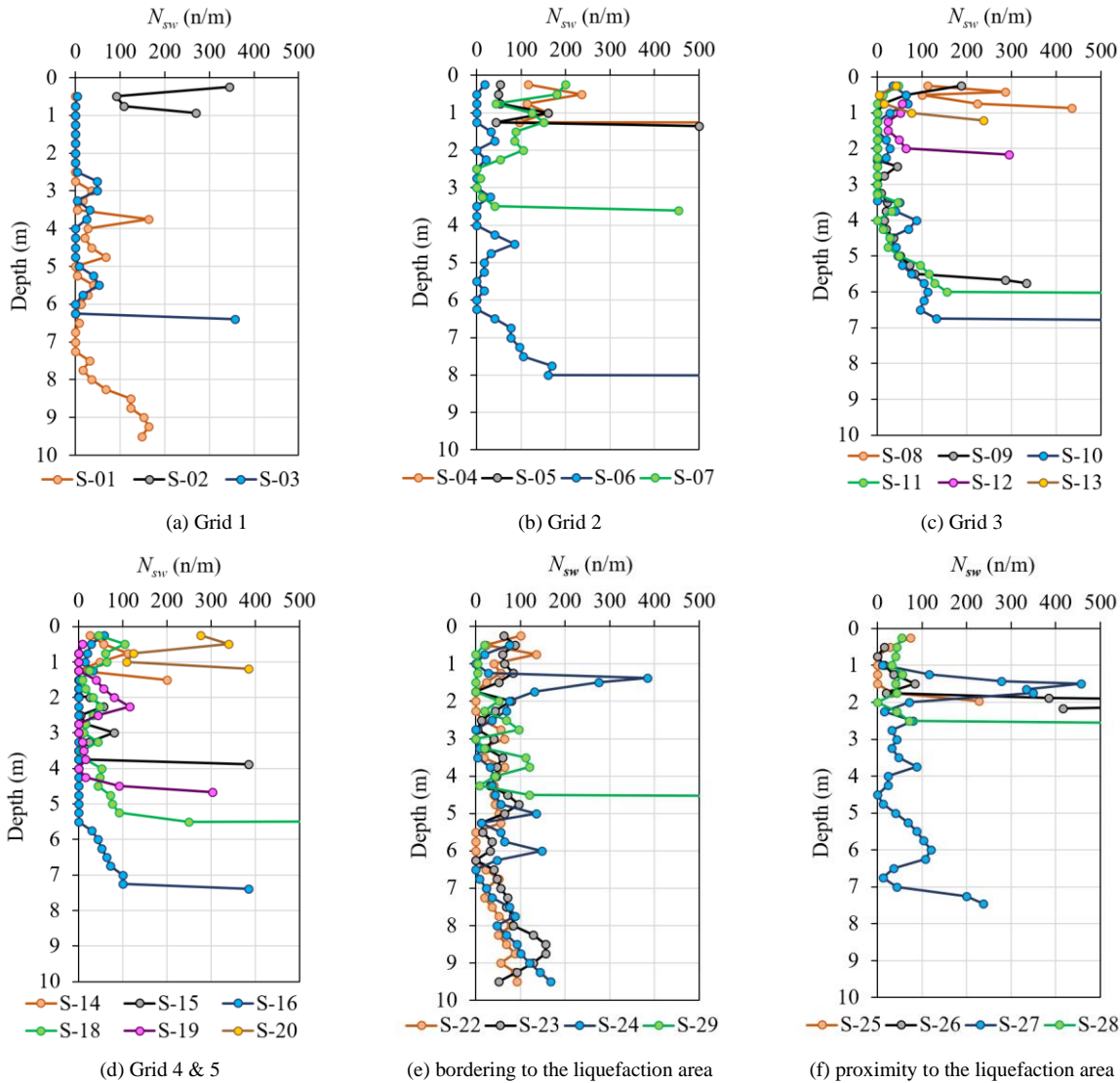


Figure 7. Charts of correlation between N_{sw} and penetration

Each test point exhibited a distinct range of N_{sw} values. Based on the observation during the test, it was noted that there were multiple points in the initial testing with relatively high N_{sw} values. Nevertheless, the values declined at the subsequent depth. During the test, the number of half-turns fell short of 50, and the penetration did not exceed a depth of 25 cm due to obstacles and the audible impact of the device colliding with rocks. In general, the tests failing to reach a depth of 9.5 had very high N_{sw} values at the end of testing due to obstructing rocks at the tip of the rods. As a result, the number of half-turns reached 50 with penetration merely reaching less than 25 cm. If the screw point encounters rocks, pebbles, or dense dirt during penetration, the SWS handle may become rigid. In contrast, if the screw point is unimpeded by rocks and the rods fail to penetrate, the handle can be easily rotated.

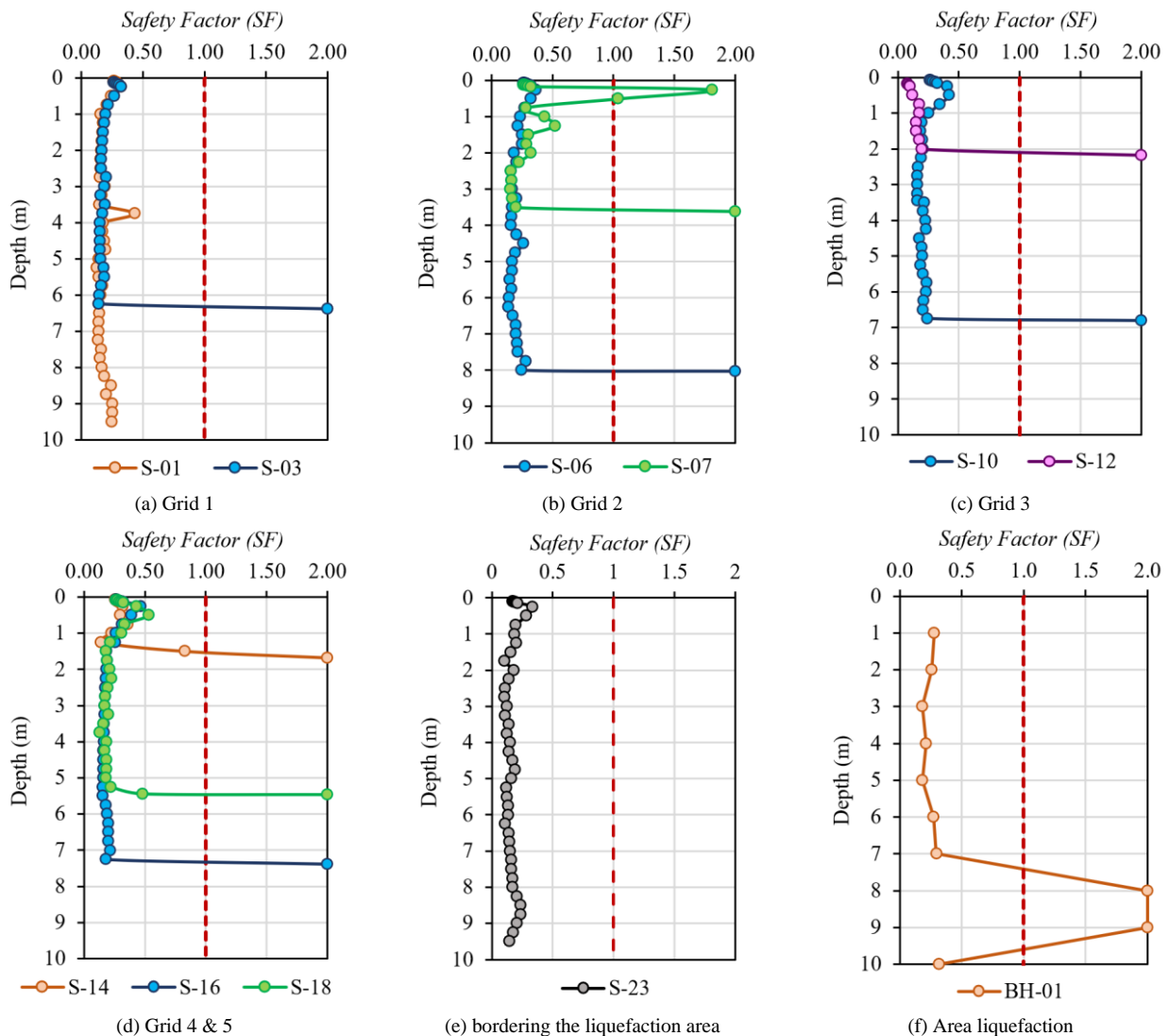
4.5. Results of Liquefaction Potential Analysis

The liquefaction potential was analyzed based on the results of 6 borehole locations from USGS [7], including BH-01, BH-02, BH-03, BH-04, BH-05, and BH-06 and 10 points of SWS tests including S-01, S-03, S-06, S-07, S-10, S-12, S-14, S-16, S-18, and S-23. The maximum depth of the SWS test was 9.5 m. Hence, the analysis using SPT data was exclusively performed up to a depth of 10 m.

The SWS test was conducted to acquire data on W_{sw} (amount of load) and N_{sw} (a load of half turn per meter) with depth (m). W_{sw} and N_{sw} values were converted to N values using the Inada equation [36]. This conversion aimed to analyze the liquefaction potential using N value. If the N_{sw} value is equal to zero, the N value is equal to 2 for coarse-grained soil and 3 for fine-grained soil. The SWS tests were administered on 10 specific points, which were either similar or adjacent to the position of the CPT (Cone Penetration Test). Therefore, the data of soil profiling from CPT were used to determine the soil types, weight value, and fine content (FC) for the liquefaction potential analysis.

Point S-01 and S-03 were the locations where the SWS tests reached the greatest depth. The N values at point S-01 and S-03 ranged from 2 to 12.99 and 1 to 12.45 consecutively. The SWS tests that did not meet the minimum depth requirement had high N_{sw} values at the end of the test. Hence, the N values obtained were also high. The N values at point S-03 ranged from 2 to 5.48. At a depth of 6.39 m, the N value reached 37.89. The N values at point S-06 ranged from 2 to 13.26. At a depth of 8.03 m, the N value was recorded at 113.67. The N values at point S-07 ranged from 2 to 14.06. In a depth of 3.61 m, the N value reached 47.69. The N values at point S-10 ranged from 2 to 10.84. At a depth of 6.81 m, the N value was recorded at 57.83. The N values on point S-12 ranged from 2 to 6.29. At a depth of 2.17 m, the N value reached 21.56. The N values at point S-14 ranged from 2 to 15.40. At a depth of 1.68 m, the N value was recorded at 20.61. The N values at point S-16 ranged from 2 to 8.70. At a depth of 7.38 m, the N value reached 40.65. The N values at point S-18 ranged from 2 to 18.75. At a depth of 5.47 m, the N value was recorded at 85.75.

Figure 8 displays the computed liquefaction potential (safety factor) values. The grid division in the SWS test can be seen in Figure 3. A $SF < 1.0$ indicates soil that is capable of liquefaction. A $SF = 1.0$ indicates soil that is in a critical condition. A $SF > 1.0$ showed soil that is not susceptible to liquefaction. The liquefaction potential analysis revealed that 10 data points from the SWS tests were categorized as SE (soft soil). The analysis was performed in an area affected by liquefaction, specifically involving sites S-01, S-03, S-06, S-07, S-10, S-12, S-14, S-16, S-18, as well as an undamaged area represented by site S-23. The $SF > 1.0$ values were obtained from the final depth of SWS testing, which did not reach the maximum depth of 9.5 m. The penetration at point B7 reached depths of 0.25 and 0.5 m, with corresponding values of 1.81 and 1.04, respectively. The $SF < 1.0$ values were recorded at all depths for test points, including S-01 and S-23, which reached the maximum depth of 9.5.



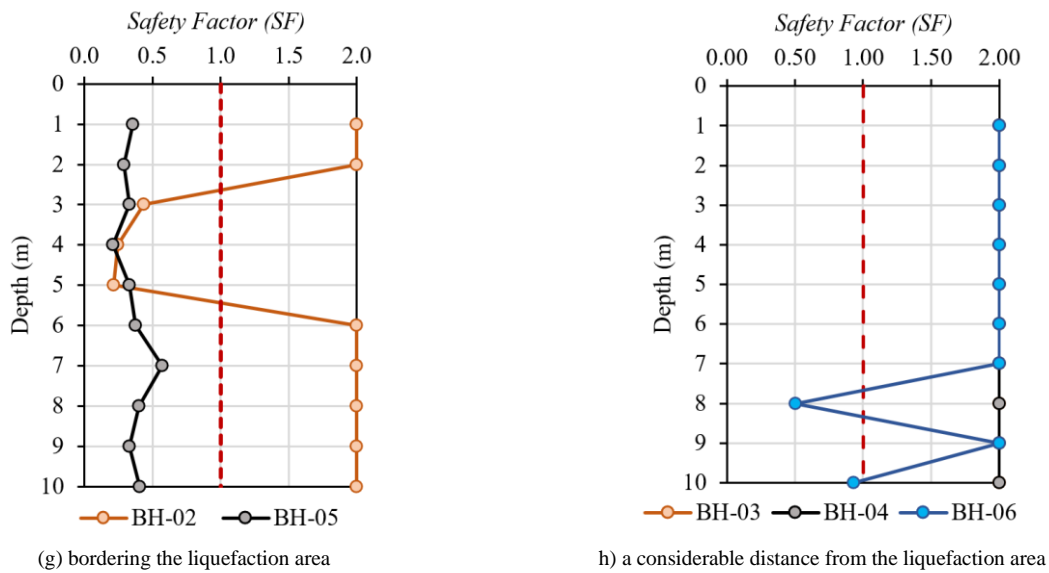


Figure 8. Charts of Safety Factor (*SF*) for penetration depth

The $SF < 1.0$ values obtained from SWS tests for each point ranged from 0.12 to 0.44 for S-01, 0.14 to 0.32 for S-03, 0.14 to 0.36 for S-06, 0.15 to 0.52 for S-07, 0.16 to 0.42 for S-10, 0.08 to 0.20 for S-12, 0.14 to 0.36 for S-14, 0.16 to 0.47 for S-16, 0.13 to 0.53 for S-18, and 0.10 to 0.48 for S-23. The liquefaction potential analysis charts based on SWS data are displayed in Figures 8a, 8b, 8c, 8d, and 8e. The liquefaction potential analysis had $SF > 1.0$ values at the end of the test, which can be attributed to the exceptionally high weight value of half turn per meter (N_{sw}) at the ultimate depth of the test. The safety factor (SF) obtained from all depths exhibited a substantial correlation with the obtained N_{sw} values, i.e., as the N_{sw} values increased, the N values also increased.

The examination of liquefaction potential, based on the Standard Penetration Test (SPT) data, revealed that the SF value was less than 1.0 for the BH-01 and BH-05 locations, which were classed as SE (soft soil). Meanwhile, $SF > 1.0$ was derived from BH-03, BH-04, and BH-06, which were classified as SD (medium soil). The investigation revealed that BH-01 and BH-05 exhibited liquefaction characteristics at all depths. BH-02 displayed a shear strength (SF) value lower than the threshold between depths of 3 m, 4 m, and 5 m. On the other hand, BH-03, BH-04, and BH-06 were found to be non-liquefiable. Table 2 displays the liquefaction potential at each test point. The $SF < 1.0$ values obtained from SPT tests for each point ranged from 0.18 to 0.32 for BH-01, 0.21 to 0.57 for BH-05, and 0.32, 0.24, and 0.15 for BH-02 at depths of 3 m, 4 m, and 5 m respectively. The liquefaction potential analysis charts based on SPT data are displayed in Figures 8f, 8g, and 8h. Research conducted in the Balaroa area using SPT data [13, 14, 17] has yielded similar results to our study. Specifically, they have found that the liquefaction-affected area has $SF < 1.0$, while sites on the steep slopes of Balaroa have $SF > 1$ [17].

According to the calculations, any future earthquake of a specific magnitude will result in liquefaction in the area that has already been damaged by liquefaction. The presence of this potential is attributed to the shallow water tables in the Balaroa area, characterized by subpar and stratified sandy soil with a fine grain and low N value. In general, the soil in the area impacted by liquefaction was not compacted, as indicated by the SWS tests where the number of half turns for a 25 cm-deep penetration did not exceed 50. In addition, 19 test spots achieved zero rotation at specific depths

4.6. Liquefaction Potential Index (*LPI*)

LPI was calculated based on the SF value to evaluate the liquefaction vulnerability of an area. The results of *LPI* analysis at 10 SWS testing points and 6 SPT testing points can be seen in Table 3. The *LPI* analysis results in Table 3 indicate that the liquefied-affected points comprising S-01, S-03, S-06, S-07, S-10, S-16, S-18, BH-01, and BH-05 are very highly vulnerable to liquefaction. Points S-12 and S-14 exhibited a high of vulnerability. The liquefaction vulnerability was very high in the vicinity of the liquefaction-affected areas S-23 and BH-02. Conversely, the number of points, i.e., BH-03 and BH-04, located far from the area was very low. BH-06 was the only point with a low level of vulnerability. Test points S-12 and S-14 exhibited a high vulnerability to liquefaction due to their shallow test depths of 2.17 m and 1.58 m, respectively. Additionally, at the end of the test, both locations had remarkably high N_{sw} values of 294.12 and 200. This occurred because, at the end of the test, there were rocks that were impenetrable to the SWS equipment. Muhanifah et al. [13] also found a very high level of vulnerability to liquefaction in liquefaction-affected areas.

Table 3. Results of Liquefaction Potential and *LPI* Value Analysis

Site Code	Site Classification	Safety Factor	Liquefaction Potential	<i>LPI</i>	Level of Potential Liquefaction
S-01	SE	$SF_{Li q} < 1.0$	Liquefaction	58.60	Very High
S-03	SE	$SF_{Li q} < 1.0$	Liquefaction	42.87	Very High
S-06	SE	$SF_{Li q} < 1.0$	Liquefaction	50.32	Very High
S-07	SE	$SF_{Li q} < 1.0$	Liquefaction	20.66	Very High
S-10	SE	$SF_{Li q} < 1.0$	Liquefaction	44.26	Very High
S-12	SE	$SF_{Li q} < 1.0$	Liquefaction	11.95	High
S-14	SE	$SF_{Li q} < 1.0$	Liquefaction	9.49	High
S-16	SE	$SF_{Li q} < 1.0$	Liquefaction	47.05	Very High
S-18	SE	$SF_{Li q} < 1.0$	Liquefaction	35.70	Very High
S-23	SE	$SF_{Li q} < 1.0$	Liquefaction	56.15	Very High
BH-01	SE	$SF_{Li q} < 1.0$	Liquefaction	46.37	Very High
BH-02	SD	$SF_{Li q} > 1.0$	No Liquefaction	18.15	Very High
BH-03	SD	$SF_{Li q} > 1.0$	No Liquefaction	0.00	Very Low
BH-04	SD	$SF_{Li q} > 1.0$	No Liquefaction	0.00	Very Low
BH-05	SE	$SF_{Li q} < 1.0$	Liquefaction	46.97	Very High
BH-06	SD	$SF_{Li q} > 1.0$	No Liquefaction	4.61	Low

The liquefaction potential and *LPI* analyses showed relevant results regarding 10 SWS testing points and 5 SPT testing points, including BH-01, BH-03, BH-04, BH-05, and BH-06. Meanwhile, the analysis identified BH-02 as having a very high vulnerability, as shown by $SF < 1.0$ only at depths ranging from 3 to 5 m with *SF* values comprising 0.32, 0.24, and 0.15. The *LPI* analysis results were used to create a map of liquefaction vulnerability using ArcGIS software. The liquefaction vulnerability on the geological surface of Balara was classified into four categories, namely very high, high, low, and very low, as shown in Figure 9. This map can serve as a reference for local governments in making regulations on land use and liquefaction risk-based building criteria.

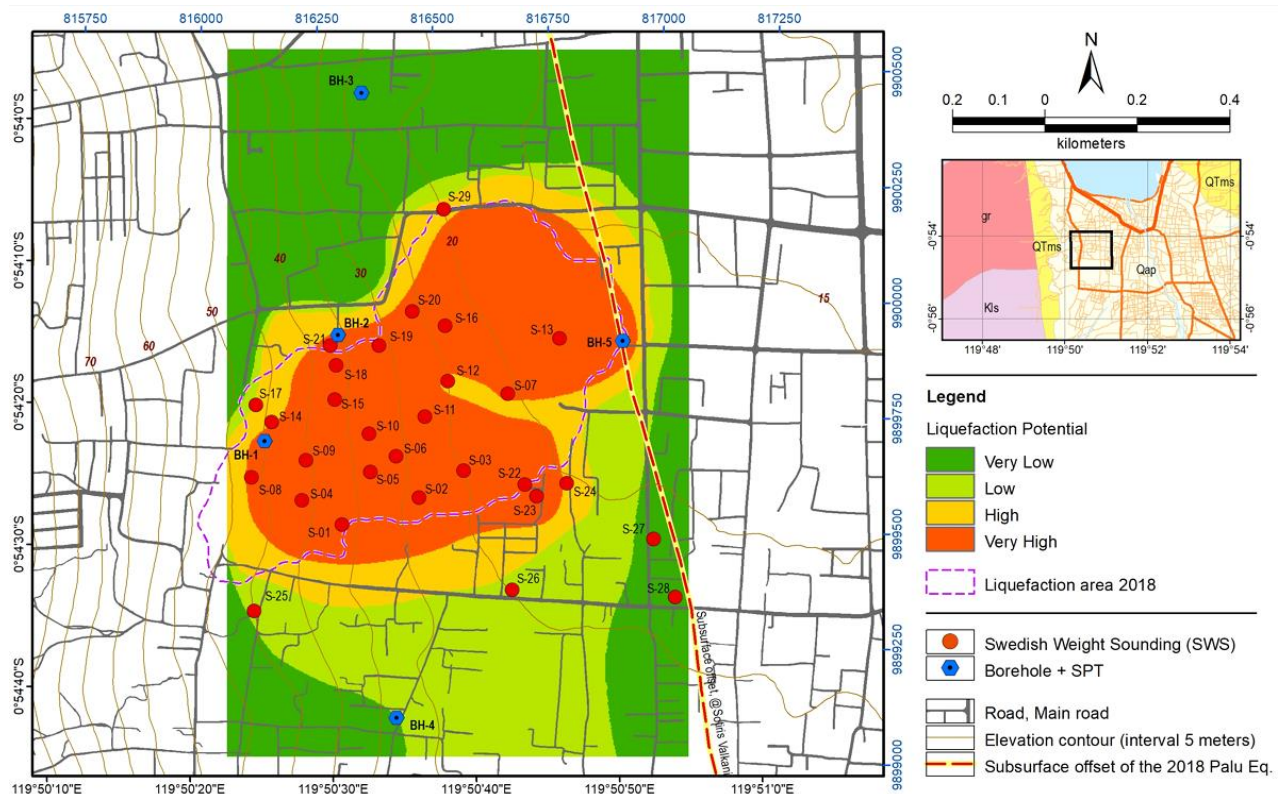


Figure 9. Map of Liquefaction Vulnerability in Balara Area

5. Conclusions

In Balaroa, the liquefied area is covered with an abundance of grass, and even certain sections have transformed into marshland, with the growth of tall grass. Through visual examination, the water tables in the liquefied area were extremely shallow, as several sections were filled with water despite the extremely hot temperature. In addition, the field test results indicated that all points of the SWS test have shallow water, with depths ranging from 5 to 60 cm.

The liquefaction potential analysis applied the N -SPT equation to convert the N_{sw} value and W_{sw} value to the N value. The N values of the 10 test points varied between 2 and 18.75 for the number of half-turns less than 50 and between 20.61 and 113.67 for the number of half-turns greater than or equal to 50. The N value obtained from the conversion results was lower than that of the SPT results. The results of liquefaction potential analysis using the SWS data revealed that the $SF < 1.0$ in all 10 test points, except those that did not meet the maximum depth of 9.5 m. The analysis revealed that the safety factor is lower and the LPI value is higher in SWS data compared to SPT one. Therefore, it is necessary to develop a new empirical equation that can approximate the N value obtained from SPT, as demonstrated in previous research [23].

The results of the liquefaction potential index (LPI) analysis using SWS data and SPT data indicate very high and high levels of liquefaction susceptibility, both in the affected area and near the affected area. Meanwhile, in areas relatively far from the liquefaction-affected area, using SPT data, low and very low levels of liquefaction susceptibility were obtained. This shows that the SWS data and SPT data have the same liquefaction potential analysis results, although the N values from the conversion are lower. Based on this, the results of the study indicate that liquefaction in the Balaroa area has the potential to occur again in the areas affected by liquefaction during the 2018 Palu earthquake if an earthquake of a certain magnitude occurs.

The results of LPI analysis using the SWS and SPT data indicated that the liquefaction vulnerability in all points was high and very high, whether they were within or adjacent to the affected area. Meanwhile, the examination of the SPT data showed that the risk of liquefaction in locations far from the affected area was low and very low. The results demonstrated that the liquefaction analysis results of SWS and SPT data were equivalent despite the lower converted N . In conclusion, the findings indicated that in the Balaroa region, liquefaction can return in the same area that was impacted by the earthquake in Palu in late 2018, given a certain magnitude of seismic activity.

6. Declarations

6.1. Author Contributions

Conceptualization, I., A.R., T.F.F., and A.D.A.; methodology, I., A.R., T.F.F., and A.D.A.; software, I.; validation, I., A.R., T.F.F., and A.D.A.; formal analysis, I., A.R., T.F.F., and A.D.A.; investigation, I.; resources, I.; data curation, I. and A.R.; writing—original draft preparation, I.; writing—review and editing, I., A.R., T.F.F., and A.D.A.; visualization, I.; supervision, A.R., T.F.F., and A.D.A.; project administration, I. and A.R.; funding acquisition, I. and A.R. All authors have read and agreed to the published version of the manuscript.

6.2. Data Availability Statement

The data presented in this study are available on request from the corresponding author.

6.3. Funding

This work was supported by the Final Assignment Recognition Program (RTA) of Universitas Gadjah Mada with Number 5075/UN1.P.II/Dit-Lit/PT.01.01/2023.

6.4. Acknowledgements

The author would like to thank the Final Assignment Recognition Program (RTA) of Universitas Gadjah Mada with Number 5075/UN1.P.II/Dit-Lit/PT.01.01/2023. We would also like to thank Universitas Tadulako for its support during the study and University Tadulako students for their assistance during the field investigation.

6.5. Conflicts of Interest

The authors declare no conflict of interest.

7. References

- [1] Irsyam, M., Hanifa, N. R., Djarwadi, D., & Sarsito, D. A. (2018). Palu Earthquake Study, Central Sulawesi Province. Pusat Penelitian dan Pengembangan Perumahan dan Pemukiman, Kementerian Pekerjaan Umum dan Perumahan Rakyat, Jakarta, Indonesia. (In Indonesian).
- [2] Miyajima, M., Setiawan, H., Yoshida, M., Ono, Y., Kosa, K., Oktaviana, I. S., Martini, & Irdhiani. (2019). Geotechnical damage in the 2018 Sulawesi earthquake, Indonesia. *Geoenvironmental Disasters*, 6(1), 2–9. doi:10.1186/s40677-019-0121-0.

- [3] Kramer, S. L., & Elgamal, A. W. M. (2001). Modeling soil liquefaction hazards for performance-based earthquake engineering. Pacific Earthquake Engineering Research Center, College of Engineering, University of California, Berkeley, United States.
- [4] Seed, H. B., & Idriss, I. M. (1971). Simplified Procedure for Evaluating Soil Liquefaction Potential. *Journal of the Soil Mechanics and Foundations Division*, 97(9), 1249–1273. doi:10.1061/jsfeaq.0001662.
- [5] Youd, T. L. (1973). Liquefaction, flow, and associated ground failure. Circular. doi:10.3133/cir688.
- [6] Youd, T.L., Salazar, A. F., & Wallace, R. M. (1992). Bridge damage caused by liquefaction during the 22 April 1991 Costa Rica earthquake. Tenth world Conference on Earthquake Engineering, 19-24 July, 1992, Madrid, Spain.
- [7] USGS. (2018). USGS ShakeMap of the 2018 Sulawesi earthquake. United States Geological Survey, Reston, United States. Available online: <https://earthquake.usgs.gov/earthquakes/eventpage/us1000h3p4/shakemap/intensity> (accessed on June 2024).
- [8] Hidayat, R. (2019). Correlation of geological conditions and levels of damage in Palu earthquake. *IOP Conference Series: Materials Science and Engineering*, 650(1), 012022. doi:10.1088/1757-899X/650/1/012022.
- [9] Hidayat, R. F., Kiyota, T., Tada, N., Hayakawa, J., & Nawir, H. (2020). Reconnaissance on liquefaction-induced flow failure caused by the 2018 Mw 7.5 Sulawesi earthquake, Palu, Indonesia. *Journal of Engineering and Technological Sciences*, 52(1), 51–65. doi:10.5614/j.eng.technol.sci.2020.52.1.4.
- [10] Rohit, D., Hazarika, H., Maeda, T., Sumartini, W. O., Kokusho, T., Manafi Khajeh Pasha, S., & Nurdin, S. (2021). Forensic investigation of flowslides triggered by the 2018 Sulawesi earthquake. *Progress in Earth and Planetary Science*, 8(1). doi:10.1186/s40645-021-00452-5.
- [11] Montgomery, J., Wartman, J., Reed, A. N., Gallant, A. P., Hutabarat, D., & Mason, H. B. (2021). Field reconnaissance data from GEER investigation of the 2018 MW 7.5 Palu-Donggala earthquake. *Data in Brief*, 34. doi:10.1016/j.dib.2021.106742.
- [12] Jalil, A., Fathani, T. F., Satyarno, I., & Wilopo, W. (2021). Nonlinear site response analysis approach to investigate the effect of pore water pressure on liquefaction in Palu. *IOP Conference Series: Earth and Environmental Science*, 871(1). doi:10.1088/1755-1315/871/1/012053.
- [13] Muhanifah, H., Adi, A. D., & Faris, F. (2021). Liquefaction investigation of Balaroa, Central Sulawesi on liquefied and non-liquefied areas. *IOP Conference Series: Earth and Environmental Science*, 861(5), 052039. doi:10.1088/1755-1315/861/5/052039.
- [14] Namira, S. A., Fathani, T. F., & Adi, A. D. (2023). The analysis of liquefaction potential in Balaroa area, Palu City, Central Sulawesi. 2nd International Conference on Advanced Information Scientific Development (ICAISD) 2021: Innovating Scientific Learning for Deep Communication. doi:10.1063/5.0106281.
- [15] Rahmawati, H. A., Prakoso, W. A., & Rahayu, A. (2020). Vs and CPT based evaluation of location with high liquefaction damage during 2018 Palu earthquake. *IOP Conference Series: Materials Science and Engineering*, 930(1), 012034. doi:10.1088/1757-899x/930/1/012034.
- [16] Cipta, A., Rudyanto, A., Afif, H., Robiana, R., Solikhin, A., Omang, A., Supartoyo, & Hidayati, S. (2021). Unearthing the buried Palu–koro fault and the pattern of damage caused by the 2018 Sulawesi earthquake using HVSR inversion. *Geological Society Special Publication*, 501(1), 185–203. doi:10.1144/SP501-2019-70.
- [17] Jalil, A., Fathani, T. F., Satyarno, I., & Wilopo, W. (2021). Liquefaction in Palu: the cause of massive mudflows. *Geoenvironmental Disasters*, 8(1). doi:10.1186/s40677-021-00194-y.
- [18] Silalahi, D. (2023). Study of Liquefied Soil Properties Using the Swedish Weight Sounding Test in Balaroa Village. Ph.D. Thesis, Universitas Tadulako, Palu, Indonesia. (In Indonesian).
- [19] Japan International Cooperation Agency (JICA). (2019). The Project for Development of Refional Disaster Risk Resilience Plan in Central Sulawesi in the Republic of Indonesia. Japan International Cooperation Agency (JICA), Chiyoda, Japan.
- [20] Tsukamoto, Y., Ishihara, K., & Sawada, S. (2004). Correlation between penetration resistance of Swedish weight sounding tests and SPT blow counts in sandy soils. *Soils and Foundations*, 44(3), 13–24. doi:10.3208/sandf.44.3_13.
- [21] Bergdahl, U., Broms, B. B., & Muromachi, T. (1988). Weight sounding test (WST): International reference test procedure. International Symposium on penetration testing; ISOPT-1, 20-24 March, 1988, Orlando, United States.
- [22] Habibi, M., Cheshomi, A., & Fakher, A. (2006). A case study of liquefaction assessment using Swedish Weight Sounding. 4th International Conference on Earthquake Engineering, 12-13 October, 2006, Taipei, Taiwan.
- [23] Armario, M. J. P., Folloso, M. P. V., Gargullo, J. M. B., Lu, P. A. R., & Luna, R. A. C. (2023). Swedish weight sounding test: Site investigation for a solar power facility in the Philippines. *Smart Geotechnics for Smart Societies, 2060–2065*, CRC Press, Boca Raton, United States. doi:10.1201/9781003299127-315.

- [24] Muhamad, Y., Elisabeth T., B., & S.A, N. (2020). Swedish Weight Sounding: A prospective portable soil investigation tools for liquefaction assessment of residential houses in Indonesia. *E3S Web of Conferences*, 156, 02010. doi:10.1051/e3sconf/202015602010.
- [25] Saro, N., Shimomura, S., Kawamura, M., Shiokawa, H., & Kataoka, S. (2018). Soil classification method using screw point-soil fricative sound by Swedish weight sounding. *Journal of Structural and Construction Engineering*, 83(743), 111–121. doi:10.3130/aijs.83.111.
- [26] Tiwari, B., Pradel, D., & Ajmera, B. (2018). Equations to Calculate the Undrained Shear Strength of Lacustrine Soil Deposit with Swedish Cone Equipment. *IFCEE 2018*. doi:10.1061/9780784481585.004.
- [27] BPS. (2020). West Palu District in Figures. Kota Palu, Badan Pusat Statistik Indonesia (BPS), Jakarta, Indonesia.
- [28] Kiyota, T., Furuichi, H., Hidayat, R. F., Tada, N., & Nawir, H. (2020). Overview of long-distance flow-slide caused by the 2018 Sulawesi earthquake, Indonesia. *Soils and Foundations*, 60(3), 722–735. doi:10.1016/j.sandf.2020.03.015.
- [29] Google Earth (2024). Google Earth Pro, Google, Mountain View, United States. Available online: <https://earth.google.com> (accessed on June 2024).
- [30] Habibi, M., Cheshomi, A., & Fakher, A. (2007). Advantages and Disadvantages of Using Swedish Weight Sounding for Liquefaction Assessment. 4th International Conference on Earthquake Geotechnical Engineering, 25-28 June, 2007, Thessaloniki, Greece.
- [31] Pitts, J. (1990). The use of Swedish ram sounding and weight sounding in residual soils and weathered rocks. *Geological Society, London, Engineering Geology Special Publications*, 6(1), 161-171. doi:10.1144/GSL.ENG.1990.006.01.17.
- [32] Clayton, C. R. I., Matthews, M. C., & Simons, N. E. (1995). *Site Investigation* (2nd Edition). Wiley-Blackwell, Hoboken, United States.
- [33] Taylor, M. L., & Cubrinovski, M. (2011). Preliminary assessment of liquefaction in urban areas following the 2010 Darfield Earthquake. *Proceedings of the Ninth Pacific Conference on Earthquake Engineering: Building an Earthquake-Resilient Society*, 14-16 April, 2011, Auckland, New Zealand.
- [34] Orense, R. P., Mirjafari, Y., & Suemasa, N. (2019). Screw driving sounding: A new test for field characterisation. *Geotechnical Research*, 6(1), 28–38. doi:10.1680/jgere.18.00024.
- [35] Tsukamoto, Y., Hyodo, T., & Hashimoto, K. (2016). Evaluation of liquefaction resistance of soils from Swedish weight sounding tests. *Soils and Foundations*, 56(1), 104–114. doi:10.1016/j.sandf.2016.01.008.
- [36] Inada, M. (1960). Use of Swedish weight sounding test. *Soils and Foundations*, 8(1), 13–18.
- [37] Idriss, I. M., & Boulanger, R. W. (2008). *Soil liquefaction during earthquakes*. Earthquake Engineering Research Institute, Oakland, United States.
- [38] Mase, L. Z. (2018). Reliability Study of the Liquefaction Analysis Method Using SPT Due to the 8.6 Mw Earthquake, 12 September 2007 in the Coastal Area of Bengkulu City. *Jurnal Teknik Sipil*, 25(1), 53. doi:10.5614/jts.2018.25.1.7.
- [39] Luna, R., & Frost, J. D. (1998). Spatial Liquefaction Analysis System. *Journal of Computing in Civil Engineering*, 12(1), 48–56. doi:10.1061/(asce)0887-3801(1998)12:1(48).
- [40] Iwasaki, T., Tokida, K., & Tatsuoka, F. (1981). Soil liquefaction potential evaluation with use of the simplified procedure. *First International Conferences on Recent Advances in Geotechnical Earthquake Engineering and Soil Dynamics*, 26 April- 3 May, 1981, St. Louis, United States.
- [41] Iwasaki, T., Arakawa, T., & Tokida, K. I. (1984). Simplified procedures for assessing soil liquefaction during earthquakes. *International Journal of Soil Dynamics and Earthquake Engineering*, 3(1), 49–58. doi:10.1016/0261-7277(84)90027-5.
- [42] Iwasaki, T. (1986). Soil liquefaction studies in Japan: state-of-the-art. *Soil Dynamics and Earthquake Engineering*, 5(1), 2–68. doi:10.1016/0267-7261(86)90024-2.
- [43] Tatsuoka, F., Iwasaki, T., Tokida, K.-I., Yasuda, S., Hirose, M., Imai, T., & Kon-No, M. (1980). Standard Penetration Tests and Soil Liquefaction Potential Evaluation. *Soils and Foundations*, 20(4), 95–111. doi:10.3208/sandf1972.20.4_95.
- [44] Toprak, S., & Holzer, T. L. (2003). Liquefaction Potential Index: Field Assessment. *Journal of Geotechnical and Geoenvironmental Engineering*, 129(4), 315–322. doi:10.1061/(asce)1090-0241(2003)129:4(315).
- [45] Hayati, H., & Andrus, R. D. (2008). Liquefaction Potential Map of Charleston, South Carolina Based on the 1886 Earthquake. *Journal of Geotechnical and Geoenvironmental Engineering*, 134(6), 815–828. doi:10.1061/(asce)1090-0241(2008)134:6(815).
- [46] SNI 03:1726:2019. (2019). *Procedures for Earthquake Resistance Planning for Building and Non-Building Structures*. Badan Standardisasi Nasional, Jakarta, Indonesia. (In Indonesian).

- [47] Pusgen. (2021). Indonesian Design Response Spectrum Application 2021 Directorate General of Human Settlements. Kementerian PUPR. Available online: <https://rsa.ciptakarya.pu.go.id/2021/> (accessed on June 2024). (In Indonesian).
- [48] Youd, T. L. (2003). 70 Liquefaction mechanisms and induced ground failure. *International Handbook of Earthquake and Engineering Seismology*, 1159–1173, Elsevier, Amsterdam, Netherlands. doi:10.1016/s0074-6142(03)80184-5.
- [49] Soekamto, R. A. B., Sumadirdja, H., Suptadar, T., Hardjoprawiro, S. & Sudana, D. (1973). Palu Sheet Geological Map, Scale 1: 250,000, Sulawesi. Housing and Settlement Research and Development Center, Geological Research and Development Agency, Bandung, Indonesia. (In Indonesian).
- [50] Tadulako Geoexploring Service. (2022). Geoelectrical Measurement Report Wenner Configuration Liquefaction Location, Balaroa Village, Palu City. Tadulako Geoexploring Service, Indonesia. (In Indonesian).